

Do biological molecular machines act as Maxwell's demons?

Michał Kurzynski^a and Przemysław Chelminiak^b

Faculty of Physics, A. Mickiewicz University, Umultowska 85, 61-614 Poznań, Poland

Abstract. The nanoscopic isothermal machines are not only free energy but also information transducers. We show that the generalized fluctuation theorem with information creation and entropy reduction can be fulfilled for the enzymatic molecular machines with the stochastic dynamics which offers a choice of the work performance in variety of ways. A particular model of such dynamics is investigated. The main conclusion of the study is that the free energy processing has to be distinguished from the organization processing. From the former point of view, Maxwell's demon utilizes entropy reduction ultimately for the performance of work, whereas from the latter, which can be the case of biological molecular machines, only for the creation of information. From a broader biological perspective, three suppositions could be of especial importance: (i) a possibility of the choice is characteristic for many intrinsically disordered proteins, (ii) it takes place in the long lasting transient stage before completing the free energy transduction cycle, and (iii) a partial compensation of entropy production by information creation is the reason for most protein machines to operate as dimers or higher organized structures.

PACS. 0 5.70.Ln, 87.15.H-, 87.15.Ya, 89.75.Hc

1 Introduction

In the intention of its creator [1], Maxwell's demon was thought to be an intelligent being, able to perform work at the expense of the entropy reduction of a closed operating system. The perplexing notion of the demon's intelligence was formalized in terms of memory and information processing by Szilard [2], Landauer [3] and subsequent followers [4,5,6], who pointed out that, in order for the total system to obey the second law of thermodynamics, the entropy reduction should be compensated for by, at least, the same entropy increase, related to the demon's information gain on the operating system's state.

The present, almost universal consensus on this issue is expressed in terms of the feedback control [7,8,9,10,11,12]. First, information is transferred from the operating system to memory in the process of measurement (observation) and next, when the system is externally loaded, the transfer of information from memory to the operating system controls the work performance process, fig. 1. Following Landauer's principle, the memory content must be erased at the expense of some entropy production. It should be stressed that the information transfer may [13] but must not be related to energy transfer.

A non-informational formulation of the problem was proposed by Smoluchowski [14] and popularized by Feynman [15] as the ratchet and pawl machine. It can operate only in agreement with the second law, at the expense of

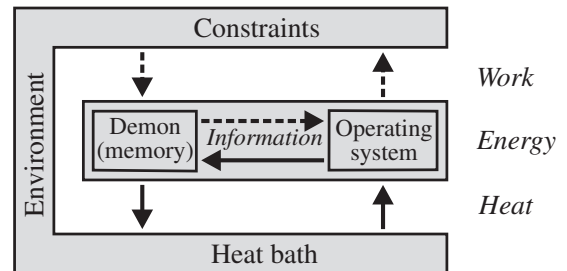


Fig. 1. Feedback control in Maxwell's demon. Entropy reduction (the heat absorption) is related to information creation but information erasing is related to entropy production (the heat emission). Note that the information transfer must not be described in energy terms so that the operating system and the memory are treated as an energetic unit. When the system is not externally loaded, no energy and information is transmitted through the broken-line arrows.

an external energy source [16]. A. F. Huxley [17] and consequent followers [18] adopted this way of thinking to suggest numerous ratchet mechanisms for the protein molecular machines' action, but no entropy reduction takes place for such models [19]. More general models of protein dynamics have been put forward [20,21,22,23,24,25,26,27,28,29] with a number of intramolecular states organized in a network of stochastic transitions. Here we show that if such models offer work performance in a variety of ways [29], the generalized fluctuation theorem [7,8,9,10,11,12,13,30,31,32] is fulfilled with possible entropy reduction. The hypothetical computer model of the network is stud-

^a e-mail: kurzphys@amu.edu.pl

^b e-mail: geronimo@amu.edu.pl

ied, displaying, like networks of the systems biology [33, 34], a transition from the fractal organization on a small length-scale to the small-world organization on the large length-scale.

We start in sects. 2 and 3 from the general theory of free energy transduction in mesoscopic isothermal machines and the relationship between the entropy and information production. Then, in sects. 4 and 5, we present the protein molecular machines as isothermal chemochemical machines and state a particular model of the protein's stochastic dynamics. Study of this model using computer simulations leads us in sect. 6 to the conclusion, that the free energy transduction in the fluctuating systems must be distinguished from the organization transduction. The latter, related to the information creation, takes place in the transient stage before completing the free energy transduction cycle, which, in the case of protein machines, can last quite long. Some biological as well as general physical implications of this statement are the subject of the concluding sects. 7 and 8.

2 Stationary isothermal machines

Long story made up for it, that the word 'machine' has several different meanings in most European languages. In our context, we understand a machine to be any physical system that enables two other systems to perform work on each other. The biological molecular machines are proteins that operate under isothermal conditions, for which the internal energy is clearly divided into the free energy and the bound energy (the entropy multiplied by the temperature), and hence, are referred to as free energy transducers [35]. The energy processing pathways in any stationary isothermal machine [36] are shown in fig. 2, where the notation of the physical quantities being in use is also explained. The thermodynamic variables X_1 and X_2 may be mechanical – displacements, electrical – charges, or chemical – numbers of distinguished molecules, hence the fluxes J_1 and J_2 may be velocities and electrical or chemical current intensities. The conjugate forces are then the mechanical forces or the differences of electrical or chemical potentials, respectively. It is important that the thermodynamic variables to be dimensionless. Then, the fluxes are counted in the turnover numbers of the machine per unit time and the reduction ratio n between them can be clearly defined.

According to the second law of thermodynamics, the net dissipation flux (the internal entropy production rate, multiplied by the temperature), $A_1 J_1 + A_2 J_2$, must be nonnegative. However, it consists of two components. The first component, $(A_1 + nA_2)J_1$, realized when the input and output fluxes are tightly coupled and $J_2 = nJ_1$, must also be, according to the same law, nonnegative. Open to discussion is the sign of the complement $A_2(J_2 - nJ_1)$.

In the macroscopic systems, the entropy S is additive and can always be divided into the following two parts S_1 and S_2 , relating to the input and output thermodynamic variables X_1 and X_2 , respectively. As a consequence, the flux $A_2(J_2 - nJ_1)$, which corresponds to S_2 , must also be

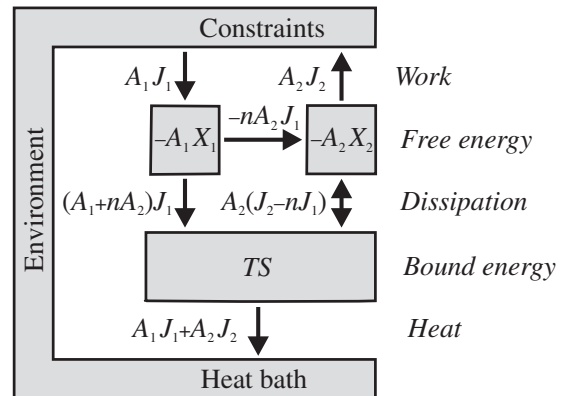


Fig. 2. Energy processing in the stationary (cyclic) isothermal machine. X_i denotes the input ($i = 1$) and the output ($i = 2$) thermodynamic variable, A_i is the conjugate thermodynamic force and the time derivative, $J_i = dX_i/dt$, is the corresponding flux. T is the temperature and S is the entropy. The constraints keep fixed stationary values of the thermodynamic variables. We assume these variables to be dimensionless, hence the forces are of energy dimension and the fluxes are counted in the turnover numbers of the machine per unit time so that the reduction ratio n between the output and input flux can be clearly defined. By convention, we assume the fluxes J_1 and J_2 to be of the same sign. Then, one system performs work on the other when the forces A_1 and A_2 are of the opposite sign. The directions of the energy fluxes shown are for $J_1, J_2, A_1 > 0$ and $A_2 < 0$. The direction of the flux, denoted by the forward-reverse arrow, is the subject of this research.

nonnegative. This means that, for negative A_2 , the output flux J_2 should not surpass more than n times the input flux J_1 . Macroscopically, the second component of the dissipation flux has the obvious interpretation of a slippage in the case of the mechanical machines, a leakage in the case of pumps, or a short-circuit in the case of the electrical machines. However, because of nonvanishing correlations, in the mesoscopic systems like the protein molecular machines, entropy is not additive [6, 31, 32] and this could result in the partial entropy reduction. In fact, the output flux J_2 can surpass the input flux J_1 [29]. Such a surprising case was observed by Yanagida and his co-workers [37, 38], who found that the single myosin II head can take several steps along the actin filament per ATP molecule hydrolysed. Whether it changes the sign of the flux $A_2(J_2 - nJ_1)$ to the negative depends on establishing the value of the reduction ratio n , which is not a simple task in the case of molecular machines, and will be discussed in detail in the next section.

From the point of view of the output force A_2 , subsystem 1 carries out work on subsystem 2 while subsystem 2 carries out work on the environment. Jointly, flux of the resultant work (the resultant power) $A_2(J_2 - nJ_1)$ is driven by the force A_2 . The complement is the flux $(A_1 + nA_2)J_1$ driven by the force $A_1 + nA_2$. Consequently, the free energy processing from fig. 2 can be alternatively presented as in fig. 3, with the free energy transduction path absent. Here, the subsystems described by two variables X_1 and $X_2 - nX_1$, respectively, are energetically independent.

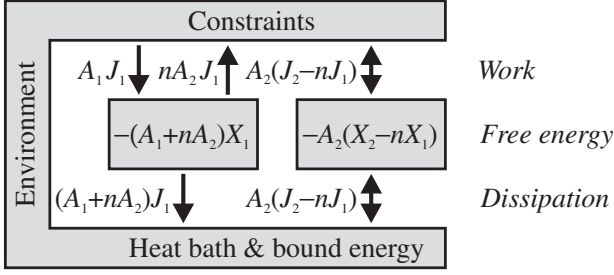


Fig. 3. Alternative view of free energy processing in the stationary isothermal machine. Here both thermodynamic variables X_1 and $X_2 - nX_1$ are energetically independent. We still study the direction of the flux denoted by the forward-reverse arrow.

However, like the subsystems described by two variables X_1 and X_2 , they are still statistically correlated,

3 Generalized fluctuation theorem

In the mesoscopic machines, the work, dissipation and heat are fluctuating variables and their variations, proceeding forward and backward in time, are related to each other by the fluctuation theorem [30,31]. In fact, the feedback control description of Maxwell's demon action [7,8,9,10,11,12], presented in fig. 1, was based on the fluctuation theorem. For the stationary process, the probability distribution function for the input and output fluxes, in general, depending on the time period t of determination, satisfies the stationary fluctuation theorem in the Andrieux-Gaspard form [39]:

$$\frac{p(j_1(t), j_2(t))}{p(-j_1(t), -j_2(t))} = \exp \beta [A_1 j_1(t) + A_2 j_2(t)] t. \quad (1)$$

This can be equivalently rewritten as the Jarzynski equality [40]

$$\langle \exp(-\sum_i \beta A_i \mathcal{J}_i(t)) \rangle = \langle \exp(-\sigma) \rangle = 1. \quad (2)$$

$\beta = 1/k_B T$, where k_B is the Boltzmann constant, p is the joint probability distribution function for the statistical ensemble of the fluxes, and $\langle \dots \rangle$ is the average over that ensemble. $\mathcal{J}_i(t)$ denotes the random variable of the mean net flux over the time period t , $i = 1, 2$, and $j_i(t)$ denotes the particular value of that flux. Time t must be long enough for the considered ensemble to comprise only stationary fluxes. σ has the meaning of a fluctuating dimensionless entropy production, and concavity of the exponential function provides the second law of thermodynamics,

$$\langle \sigma \rangle \geq 0, \quad (3)$$

to be a consequence of (2).

In further discussion, for brevity, we will omit the argument t specifying all the fluxes. In the context of the transition from fig. 2 to fig. 3, the two-dimensional probability distribution function $p(j_1, j_2)$ can be treated as a

two-dimensional probability distribution function of two variables j_1 and $j_2 - nj_1$, with $j_2 - nj_1$ as a whole treated as a single variable. If we calculate the marginal probability distributions, then, from the fluctuation theorem (1) for the total entropy production in both the fluxes j_1 and j_2 , the generalized fluctuation theorems for j_1 and the difference $j_2 - nj_1$ follow, respectively, in the logarithmic form:

$$\ln \frac{p(j_1)}{p(-j_1)} = \beta(A_1 + nA_2)j_1 t + \beta A_2 \langle (\mathcal{J}_2 - n\mathcal{J}_1)t \rangle - \left\langle \ln \frac{p(\mathcal{J}_2 - n\mathcal{J}_1 | j_1)}{p(-\mathcal{J}_2 + n\mathcal{J}_1 | -j_1)} \right\rangle \quad (4)$$

(the averages are taken over the ensemble of the flux differences $j_2 - nj_1$) and

$$\ln \frac{p(j_2 - nj_1)}{p(-j_2 + nj_1)} = \beta A_2 (j_2 - nj_1) t + \beta(A_1 + nA_2) \langle \mathcal{J}_1 t \rangle - \left\langle \ln \frac{p(\mathcal{J}_1 | j_2 - nj_1)}{p(-\mathcal{J}_1 | -j_2 + nj_1)} \right\rangle \quad (5)$$

(the averages are taken over the ensemble of the fluxes j_1). Above, we introduced conditional probabilities.

The first components on the right of eqs. (4) and (5) describe the entropy production, now only in the separate fluxes j_1 and $j_2 - nj_1$, respectively, but the interpretation of the remaining components is not so easy. The problem is that for the stationary processes, as opposed to the transient nonequilibrium protocols considered in refs. [7,8,9,10,11,12,13,31,32], the notion of the mutual information is not well defined [12].

This disadvantage may, however, be used for determination of the reduction ratio n . If it is chosen such that the remaining terms in eq. (4) cancel each other and only the entropy production term remains:

$$\ln \frac{p(j_1)}{p(-j_1)} = \beta(A_1 + nA_2)j_1 t, \quad (6)$$

then eq. (5) for the flux $j_2 - nj_1$ can be rewritten in terms of the mutual information differences:

$$\ln \frac{p(j_2 - nj_1)}{p(-j_2 + nj_1)} = \beta A_2 (j_2 - nj_1) t - \left\langle \ln \frac{p(\mathcal{J}_1 | j_2 - nj_1)}{p(\mathcal{J}_1)} \right\rangle + \left\langle \ln \frac{p(-\mathcal{J}_1 | -j_2 + nj_1)}{p(-\mathcal{J}_1)} \right\rangle. \quad (7)$$

The replacement of (4) by (6) is a complete asymmetrical coarse graining [12] of the fluxes j_1 and $j_2 - nj_1$, and can be considered as the condition for j_1 to be a hidden thermodynamic variable, from which and to which the information does not flow [41,42,43]. Like the antecedent entropic term, both the fluctuating averages in eq. (7) depend only on single variable $j_2 - nj_1$. They represent the difference of the mean information which the fluctuating flux $\mathcal{J}_2 - n\mathcal{J}_1$ sends outside to the hidden variable when proceeding, respectively, in the forward and reverse directions. Accordingly, the whole second component in eq. (7)

has the direct interpretation of the information production by the flux $\mathcal{J}_2 - n\mathcal{J}_1$ and is positive.

To conclude this section, we write the fluctuation theorem for the flux \mathcal{J}_1 , eq. (6), in the form analogous to the Jarzynski equality (2):

$$\langle \exp(-\sigma) \rangle = 1, \quad (8)$$

from which the second law inequality (3) follows. However, the Jarzynski equality for the flux $\mathcal{J}_2 - n\mathcal{J}_1$, eq. (7), should be written in the generalized form [7,8,9,10,11,12,13,31,32]:

$$\langle \exp(-\sigma - \iota) \rangle = 1, \quad (9)$$

from which the generalized second law inequality follows:

$$\langle \sigma \rangle + \langle \iota \rangle \geq 0. \quad (10)$$

As in (8), σ has the meaning of a dimensionless entropy production, while the additional quantity ι has the meaning of the information production in nats (the natural logarithm is used instead of the binary logarithm). We proved that $\langle \iota \rangle$ is positive but there is still not clear whether the entropy production $\langle \sigma \rangle$ can be negative and the general question stated in section 2 remains open. We try to answer it in the particular case of protein molecular machines.

4 Chemochemical machines. Dynamics of proteins

The relation between the output and input fluxes in protein molecular machines was the topic of our previous studies [28,29]. From a theoretical point of view, it is convenient to treat all protein machines as chemochemical machines [36]. The protein chemochemical machines are enzymes, that simultaneously catalyze two effectively unimolecular reactions: the free energy-donating input reaction $R_1 \leftrightarrow P_1$ and the free energy-accepting output reaction $R_2 \leftrightarrow P_2$, fig. 4a. Also pumps and molecular motors can be treated in the same manner. Indeed, the molecules present on either side of a biological membrane can be considered to occupy different chemical states, fig. 4b, whereas the external load influences the free energy involved in binding the motor to its track, fig. 4c, which can be expressed as a change in the effective concentration of this track [21,28,36].

The system considered consists of a single enzyme macromolecule, surrounded by a solution of its substrates, possibly involving the track. It is an open system with constraints controlling the numbers of incoming and outgoing molecules and, in particular, the number of steps performed by the motor along the track, fig. 4. Under specified relations between the concentration of the substrates [29], two independent stationary (nonequilibrium) molar concentrations of the products $[P_1]$ and $[P_2]$, related to the enzyme total concentration $[E]$, are to be treated as the input and output dimensionless thermodynamic variables X_1 and X_2 , respectively, considered in fig. 1. The

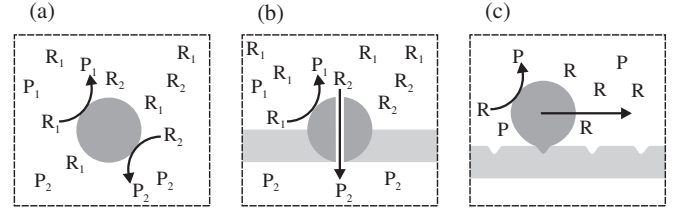


Fig. 4. Simplified representation of three types of the biological molecular machines: (a) enzymes that simultaneously catalyze two reactions, (b) pumps, and (c) motors. Constraints are symbolized by the frame of the broken line.

fluxes J_i with the conjugate thermodynamic forces A_i are determined as [35,36]

$$J_i = \frac{d}{dt} X_i = \frac{d}{dt} \frac{[P_i]}{[E]}, \quad \beta A_i = \ln \frac{[P_i]^{\text{eq}} [R_i]}{[R_i]^{\text{eq}} [P_i]}, \quad (11)$$

where the superscript eq denotes the corresponding equilibrium concentrations.

On the mesoscopic level, the dynamics of a particular biological chemochemical machine is the Markov process described by a system of master equations, determining a network of conformational transitions that satisfy the detailed balance condition [20,21,22,23,24,25,26,27,28,29,44,45,46], and a system of pairs of distinguished states (the ‘gates’) between which the input and output chemical reactions force transitions, that break the detailed balance [28,29], fig. 5(a). Recently, we proved analytically [29] that, for a single output gate, when the enzyme has no opportunity for any choice, the ratio J_2/J_1 cannot exceed one. This case also includes the various ratchet models [18], which assume the output and input gates to coincide. The output flux J_2 can only exceed the input flux J_1 in the case of many output gates, what seems to be the rule rather than exception [20,47,48,49,50,51].

Our goal is to consider the biological molecular machines with such dynamics. However, very poor experimental support is available for actual conformational transition networks in native proteins. That is why we restrict our attention to a model network here. Various models of the networks with several succeeding output gates have been considered [29] but the class of models seems to be the most realistic, based on a hypothesis that the protein conformational transition networks, like the higher level biological networks: the protein interaction network and the metabolic network, have evolved in the process of a self-organized criticality [52,53]. Such networks are scale-free and display a transition from the fractal organization on the small length-scale to the small-world organization on the large length-scale [33,34]. Very recently, a network, which seems to possess similar properties, was obtained in a long, 17 μs molecular dynamics simulation [54].

5 The model

In ref. [29], we have shown that the case of many different output gates was reached in a natural way on scale-free

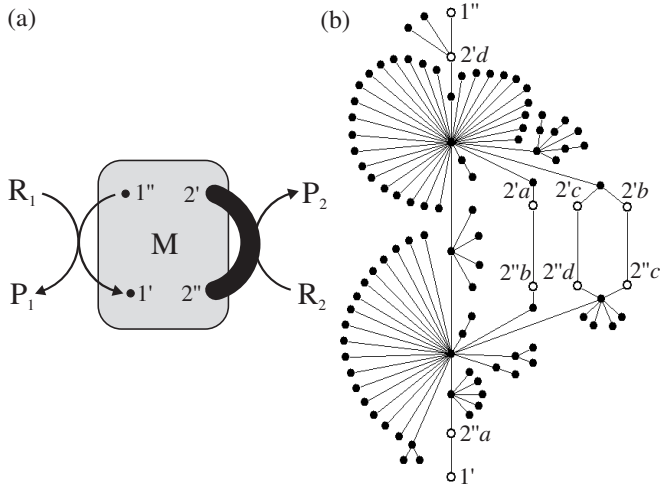


Fig. 5. Kinetics of the enzymatic chemo-chemical machine. (a) General scheme. The grey box represents an arbitrary one-component network of transitions between conformational states composing either the enzyme or the enzyme-substrates native state. All these transitions satisfy the detailed balance condition. A single pair (the ‘gate’) of conformational states $1''$ and $1'$ is distinguished, between which the input reaction $R_1 \leftrightarrow P_1$ brakes the detailed balance. Also, a single or a variety (the heavy line) of pairs of conformational states $2''$ and $2'$ is distinguished, between which the output reaction $R_2 \leftrightarrow P_2$ does the same. All the reactions are reversible; the arrows indicate the directions assumed to be forward. (b) Exemplifying realization of the 100-node network, constructed stochastically following the algorithm described in section 5. Note two hubs, the states of the lowest free energy, that can be identified with the two main conformations of the protein machine, e.g., ‘open’ and ‘closed’, or ‘bent’ and ‘straight’, usually the only occupied sufficiently high to be notable under equilibrium conditions. The single pair of the output transition states chosen for the simulations is $(2''a, 2'd)$. The alternative four output pairs $(2''a, 2'a)$, $(2''b, 2'b)$, $(2''c, 2'c)$, and $(2''d, 2'd)$, are chosen tendentially to lie one after another.

fractal trees, extended by long-range shortcuts. A network of 100 nodes with such properties is depicted in fig. 5(b). The algorithm of constructing the stochastic scale-free fractal trees was adopted after Goh et al. [55]. Shortcuts, though more widely distributed, were considered by Rozenfeld, Song and Makse [33]. Here, we chose randomly three shortcuts from the set of all the pairs of nodes distanced by six links. The network of 100 nodes in fig. 5(b) is too small to determine its scaling properties, but a similar procedure of construction applied to 10^5 nodes results in a scale-free network which is fractal on a small length-scale and a small world on a large length-scale.

To provide the network with stochastic dynamics, we assumed the probability of changing a node to any of its neighbours to be the same in each random walking step [29,56]. Consequently, the transition probability to the neighbouring node is inversely proportional to the number of links (the output node degree) and equals $(\tau_{\text{int}} p_i^{\text{eq}})^{-1}$, where p_i^{eq} denotes the equilibrium occupation probability

of the exit node. The mean internal transition time, τ_{int} , is determined by the doubled number of links, i.e., $2(100 - 1 + 3) = 204$ random walking steps for the 100 node tree network with 3 shortcuts assumed. Following the detailed balance condition, the free energy of a given node is proportional to its degree. The most stable conformational substates are the hubs. The mean first passage time between the most distant nodes we found to equal 710 random walking steps.

The forward external transition probabilities, determined by the stationary concentrations $[P_i]$, were assumed to equal $(20 p_i^{\text{eq}})^{-1}$ per random walking step, p_i^{eq} denoting the equilibrium occupation probability of the initial input or output node, $i = 1, 2$. The corresponding backward external transition probabilities were modified by the detailed balance breaking factors $\exp(-\beta A_i)$. The mean forward external transition time $\tau_{\text{ext}} = 20$ is one order of the magnitude shorter than the mean internal transition time $\tau_{\text{int}} = 204$, so that the whole process is controlled by the internal and not by the external dynamics of the system.

All the averages in the equations from (2) to (10) are to be performed over a statistical ensemble of the stationary fluxes determined for the time period t . We can get such the ensemble by dividing a long stochastic trajectory of random walk on the studied network into the segments of the length t , and next by determining the net numbers of external transitions, hence the values of the fluxes $j_1(t)$ and $j_2(t)$ for each segment. However, we have to be sure that the time period t is long enough for the considered ensemble to comprise only stationary but not transient fluxes.

Because the initial state is random in the successive divisions of the trajectory into the segments of equal length, the mean value of the flux $\langle J_i(t) \rangle$ (but not the higher moments!) coincides practically with its stationary value J_i , even for the very short time period t . To evaluate the actual mean transient time t_{tr} , after which the fluxes become stationary, we have first to divide the whole trajectory into cycles or ‘protocols’ [30,31] of transient trajectories starting and ending in the same state, say $1'$. For the ensemble of cycles of the length t , or t within a certain small range, we can determine the means $J_1(t)$ and $J_2(t)$ and in such a way find the time, after which dynamics of the studied system passes from the transient to the stationary stage.

We performed Monte Carlo simulations of random walk in 10^{10} computer steps on the network shown in fig. 5b, with both the single and the fourfold output gate. The gates were chosen tendentially to maximize the value of J_2/J_1 . We assumed $\beta A_1 = 1$ and a few smaller, negative values of βA_2 determining the ratio $\epsilon = J_2/J_1$. The presence of external transitions, breaking the detailed balance, makes some computational complications, which are discussed and explained in detail somewhere else [56].

The time dependences of the means over cycles $J_1(t)$ and $J_2(t)$, found in our model random walk simulations, will be the subject of a separate paper. Here, only the time dependence of $J_2(t)$ and $J_2(t) - J_1(t)$ for the fourfold output gate and a chosen value of the ratio J_2/J_1 is depicted in fig. 6. We do not present $J_1(t)$ and $J_2(t)$ sep-

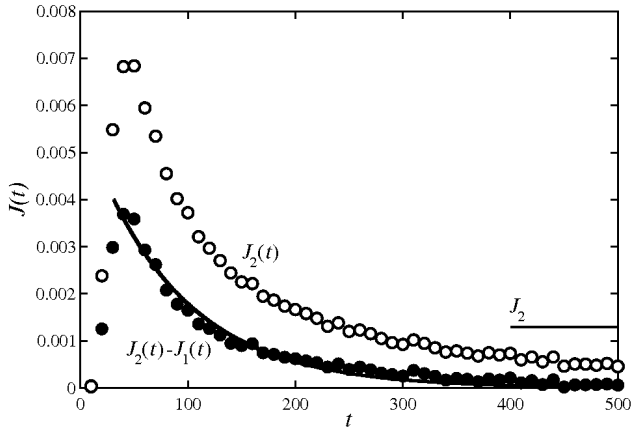


Fig. 6. Time dependence of the means over cycles $J_2(t)$ and $J_2(t) - J_1(t)$ found in the model random walk simulations on the network shown in fig. 5b with the fourfold output gate and the stationary flux ratio $J_2/J_1 = 1.59$. The solid line corresponds to exponential fitting the downfall of the flux difference $J_2(t) - J_1(t)$ to zero. The stationary value of J_2 is also quoted.

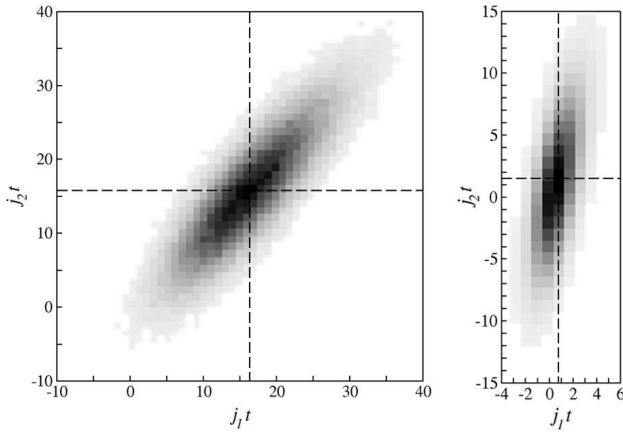


Fig. 7. Exemplifying two-dimensional probability distribution functions $p(j_1(t), j_2(t))$ found in the model random walk simulations on a network shown in fig. 5b with the single output gate (left) and the fourfold output gate (right). For the single output gate, we assumed $t = 10^4$ random walking steps and $J_2/J_1 = 0.95$. For the fourfold output gate, we assumed $t = 10^3$ random walking steps and $J_2/J_1 = 1.59$. For more details, see the text. The averaged values of the individual fluxes, multiplied by the time t of determination, are marked by the broken lines.

arately, because they tend to values completely different from the stationary values J_1 and J_2 , respectively, what means that the latters are determined mainly in stationary and not the transient stages of dynamics. Only the difference $J_2(t) - J_1(t)$ tends to zero, what is understandable because the transition through the input gate each time starts the trajectory from the initial state $1'$ and the whole contribution to the stationary difference $J_2 - J_1$ originates from the transient stage of evolution. Exponential fitting the downfall of the flux difference $J_2(t) - J_1(t)$ to zero allows us to evaluate the transient time value for

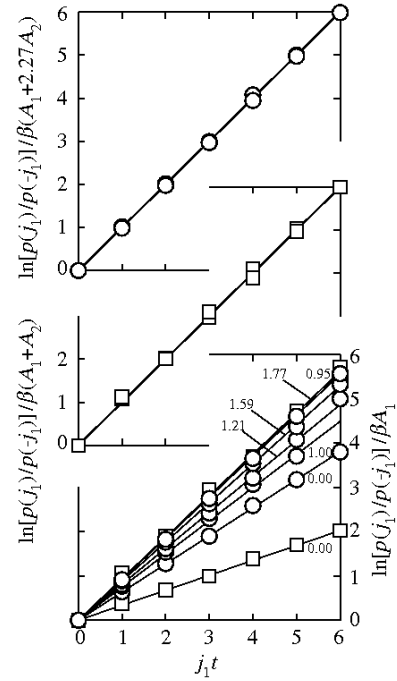


Fig. 8. Generalized fluctuation theorem dependence (4) found in the model random walk simulations. The examined network was that shown in fig. 5(b) with the single output gate (the squares) and the fourfold output gate (the circles). We assumed $\beta A_1 = 1$ and a few smaller, negative values of βA_2 determining the ratio $\epsilon = J_2/J_1$ of the average output and input fluxes noted in the figure. At the beginning, the dependence was related to the force βA_1 (the lowest diagram). Relating it to $\beta(A_1 + nA_2)$, eq. (6), allowed us to fit the value of the reduction ratio n to be 1.00 for the single output gate (the higher diagram), and 2.27 for the fourfold output gate (the highest diagram). In the last diagram, many simulation points practically cover each other.

the case of the fourfold output gate to be approximately $t_{tr} = 100$ random walking steps.

Trials with divisions of the whole trajectory into segments of different lengths led us to the conclusion that

- (i) The obtained two-dimensional probability distribution functions $p(j_1(t), j_2(t))$ satisfy the Andrieux-Gaspard fluctuation theorem (1) for t longer than the transient time t_{tr} .

To get the statistical samples of the stationary fluxes numerous enough, we choose the time of the stationary averaging $t = 10^4$ random walking steps for the single gate and $t = 10^3$ random walking steps for the fourfold gate. Exemplary two-dimensional probability distribution functions $p(j_1(t), j_2(t))$ are shown in fig. 7.

Upon analysing the results we found that

- (ii) The logarithm of the ratio of marginals $p(j_1)/p(-j_1)$ can be described by the generalized fluctuation theorem formula (4) with both the entropic and additional components linearly depending on j_1 . The correction to entropy production is negative.

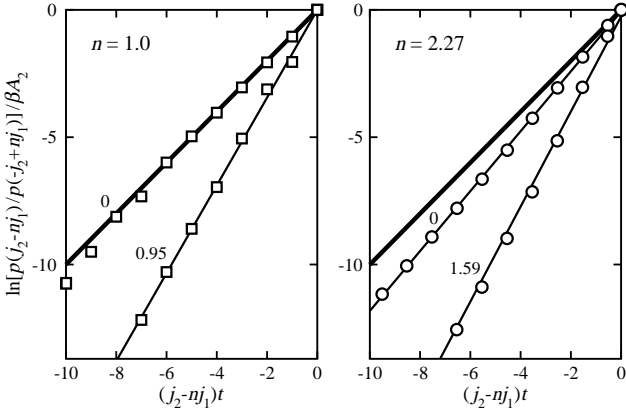


Fig. 9. Generalized fluctuation theorem dependence (7) for the marginal $j_2 - nj_1$, found in the model random walk simulation for the single ($n = 1$) and the fourfold ($n = 2.27$) output gate. Two markedly different values of the ratio $\epsilon = J_2/J_1$ were chosen for each case. Because the corresponding values of βA_2 are negative, the simulation points lie in the lower half-plane of the graph. The thick, solid line corresponds to the lack of information production in eq. (7).

The dependences of $\ln[p(j_1)/p(-j_1)]$ on $j_1 t$, when divided by βA_1 , are plotted in fig. 8 and fitting these dependences to Eq. (6) allowed us to determine the value of the reduction ratio to be $n = 1.00$ for the single output gate and $n = 2.27$ for the fourfold output gate. Knowing these values, from the two-dimensional probability distributions $p(j_1, j_2)$, we determined the marginal distributions $p(j_2 - nj_1)$ and found that

- (iii) The logarithm of the ratio of the marginals $p(j_2 - nj_1)/p(-j_2 + nj_1)$ can be described by the generalized fluctuation theorem formula (7) with both the entropic and informative components linearly depending on $j_2 - nj_1$. The informative correction is, as expected, positive.

Exemplary verifications of eq. (7) are depicted in fig. 9 both for the single and the fourfold output gate. Two markedly different values of the ratio $\epsilon = J_2/J_1$ were chosen for each case. Because the corresponding values of βA_2 were negative, the simulation points lie in the lower half-plane of the graph. The thick, solid line corresponds to the lack of information production in eq. (7). Such the case takes place for the force $\beta A_2 = -0.670$, that stalls the flux through the single output gate ($J_2/J_1 = 0$). The same effect of stalling the flux through the fourfold output gate is reached for $\beta A_2 = -0.173$, but this is accompanied by a non-zero information production (the line with a larger slope) resulting from the possibility of the choice of the output gate even if the resultant net flux is zero.

From the simulations for the fourfold output gate, we found that the stationary ratio $\epsilon = J_2/J_1$ for $\beta A_2 \leq 0$ cannot be greater than 2.01. As a consequence, because of $\epsilon < n = 2.27$, the entropy production rate

$$\beta A_2(J_2 - nJ_1) = \beta A_2(\epsilon - n)J_1 \quad (12)$$

is always positive, like the entropy production rate for the single output gate. To conclude, the direction of the

flux, denoted in figs. 2 and 3 by the forward-reverse arrow, should be forward.

6 Free energy versus organization processing

The nanoscopic machines are not only free energy but also information transducers. In other words, in nanoscopic machines 'information can serve as a thermodynamic resource similar to free energy' [19]. Two kinds of information are produced during time course of the simulated process. The first is in the form of a tape with more or less random sequence of signs $\dots ++-+-++-+-\dots$ describing directions (forward or backward) of the successive transitions through the output gate or gates. And the second, in the case of many output gates, is in the form of a tape with more or less random sequence of letters $\dots bcd d a c b b a \dots$ labelling successive gates, which the system passed through.

Both kinds of information are related to the intramolecular stochastic dynamics of the machine. This dynamics can be considered to play the role of an information reservoir or register [13], which is erased each time the system passes through the input gate and starts its evolution anew from the initial state $1'$. At that moment, the old tapes are terminated and the new tapes are initiated.

It should be pointed out that the recorded information depends crucially on the ratio of τ_{ext} to τ_{int} . The mean external transition time τ_{ext} is determined by the mechanism of the enzyme-substrates recognition and binding, and can vary within wide limits [29]. The longer τ_{ext} , i.e., the more the reaction is controlled by the external dynamics, the lower probability of the backward transition through the same gate or the forward transition through the next gate. In the limit $\tau_{\text{ext}} \gg \tau_{\text{int}}$, when the internal dynamics is negligible as in the transition state theory of the reaction rates [36], only the single external transitions forward take place and $n = 1$ also in the case of the multiple output gates.

It is impossible to determine information of the second kind experimentally, and for its theoretical determination, detailed studies of individual, successive transient protocols related to individual trajectories are needed [31, 32]. However, information of the second kind influences strongly information of the first kind, and the latter flows out of the machine and determines the number of the product molecules P_2 , hence the fluctuating variable X_2 .

Both kinds of information are erased each time the system passes forward through the input gate and the molecule P_1 is created, hence the variable X_1 increases by one. In other words, the information created by the molecular machine in the successive transient stages is written in the fluctuating number of product molecules P_2 created per product molecule P_1 , i.e., in the fluctuating variable $X_2 - X_1$ (which can differ from the variable $X_2 - nX_1$!). We know that the corresponding stationary flux $J_2 - J_1$ is determined entirely by the transient stage dynamics (fig. 6). What is more, it is positive for $\epsilon = J_2/J_1 > 1$, what, for the negative output force βA_2 , means the entropy reduction, not production.

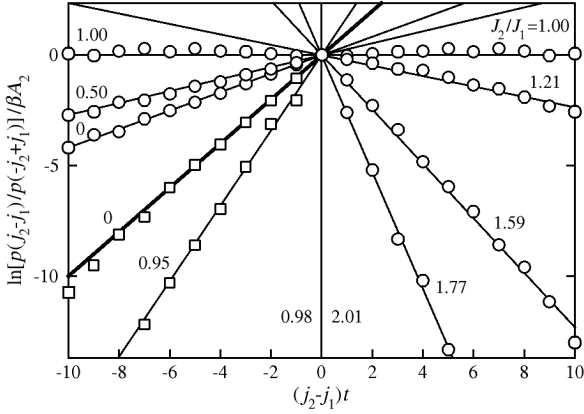


Fig. 10. Generalized fluctuation theorem dependence (5) with $n = 1$, found in the model random walk simulations. The examined network was that shown in fig. 5b with the fourfold output gate (the circles). The dynamics of the model was described in sect. 5. We assumed $\beta A_1 = 1$ and a few negative values of βA_2 determining the difference $J_2 - J_1$ of the stationary output and input fluxes (or the ratio J_2/J_1 noted in the figure). The results of each simulation were obtained symmetrically on the whole axis of the fluctuating difference $j_2 - j_1$ but in the figure, they are presented, divided by the (negative!) coefficient βA_2 , only on the left from zero for the negative average $J_2 - J_1$, and on the right from zero for the positive average $J_2 - J_1$. The thick, solid line corresponds to the lack of information production in eq. (5). Two lines for $J_2/J_1 < 1$ have lower slope, what means that the information production in the case of the fourfold output gate is negative (the information gain). For comparison, the data for the single output gate (the squares) are quoted from fig. 9a with the information loss. For the fourfold output gate, the entropy production is completely compensated for by the information gain for $\beta A_2 = -0.108$, when the average difference $J_2 - J_1$ reaches the value of 0 (the horizontal line). The slope of the line becomes negative for $J_2/J_1 > 1$, what is discussed in the text. The vertical line ($\beta A_2 = 0$) corresponds to the maximum value of J_2/J_1 both for the single ($J_2/J_1 = 0.98$) and the fourfold ($J_2/J_1 = 2.01$) output gate.

In order to determine the temporal fluctuations of the flux $J_2 - J_1$ we determined, from the two-dimensional distributions $p(j_1, j_2)$, the precisely diagonal marginals $p(j_2 - j_1)$ and found that

- (iv) The logarithm of the ratio of the diagonal marginals $p(j_2 - j_1)/p(-j_2 + j_1)$ can be described by the generalized fluctuation theorem formula (5) with $n = 1$ and all the components linearly depending on the difference $j_2 - j_1$. The informative correction can be of arbitrary sign and large.

The dependences of $\ln[p(j_2 - j_1)/p(-j_2 + j_1)]$ on $j_2 - j_1$ are depicted in fig. 10 for a few chosen negative values of βA_2 that determine the difference of the averages of the output and input fluxes $J_2 - J_1$, or the ratio of those averages, J_2/J_1 . We discarded the rare results for higher values of $j_2 - j_1$ as being burdened with statistical error too large. The simulation data are presented in such a way that the transition from the entropy production to entropy reduction might be clearly seen. The thick, solid line cor-

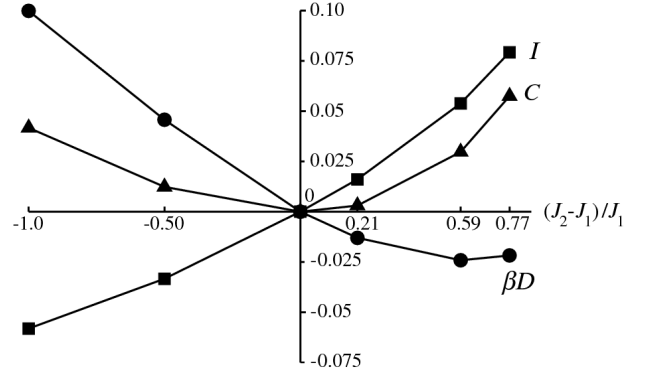


Fig. 11. Dependence of the information production I (the squares) and the entropy production βD (the circles) per $t = 10^3$ random walking steps of determination, on the flux difference $J_2 - J_1$. The points represent the values obtained from the data given in fig. 10. The sum of βD and I , we refer to as the cost C (the triangles), is also shown.

responds to the first, entropic term to the right-hand side of eq. (5). For the single output gate, when the system has no opportunity of any choice, the informative correction is zero or of the same sign as the entropic contribution (positive), that corresponds to an information loss by the flux $J_2 - J_1$ in favor of the flux J_1 . For many output gates, information gain, resulting from the possibility of a choice, surpasses the information loss and reduces the effects of the entropy production in part, until the limit of the tight coupling, $J_2 - J_1 = 0$ ($J_2/J_1 = 1$), above which information production prevails.

As for the flux $J_2 - nJ_1$, also for the flux $J_2 - J_1$ we interpret eq. (5) in terms of the second law (10):

$$\langle \sigma \rangle + \langle \iota \rangle \geq 0. \quad (13)$$

Formally, upon substituting $n = 1$ to eq. (5), the average dimensionless entropy production (the dissipation D divided by $k_B T$) is determined as

$$\beta D = \langle \sigma \rangle = \beta A_2 (J_2 - J_1) t, \quad (14)$$

whereas the average information production I , as

$$I = \langle \iota \rangle = \beta (A_1 + A_2) J_1 t + \left\langle \ln \frac{p(-J_1 | -J_2 + J_1)}{p(J_1 | J_2 - J_1)} \right\rangle. \quad (15)$$

In the last term of eq. (15), we omitted the argument t of the fluxes for brevity. The stationary values J_1 and J_2 are related to the force A_2 , so we can directly determine the average entropy production (14) for given time period t . Fig. 10 shows clearly the linear relation

$$\beta D + I = \alpha \beta D, \quad (16)$$

where α is the tangent of the adequate straight line slope. From (16), knowing βD and α , we can determine the average information production I without referring to the much more complex formula (15). The values of I and βD , obtained from the values of α found from fig. 10, are

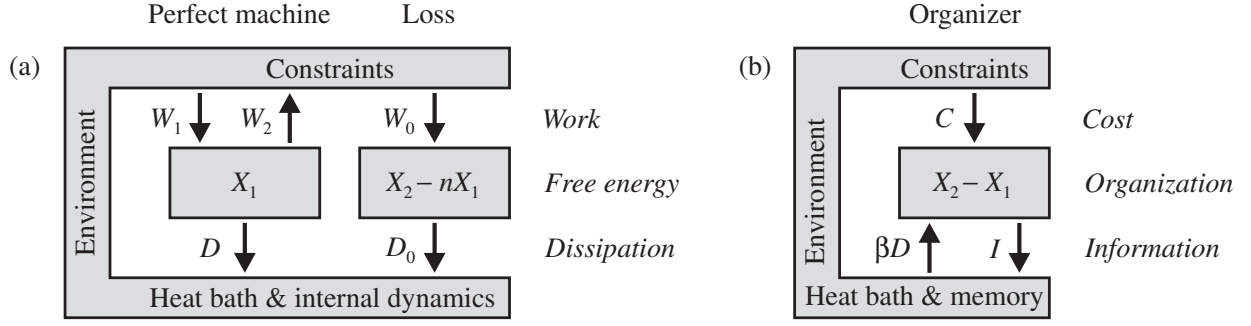


Fig. 12. Free energy (a) versus organization (b) processing in the system participating in a stationary isothermal process. The perfect free energy processing is distinguished from possible loss. See the text for more detailed discussion.

presented in fig. 11 as the functions of $J_2 - J_1$. Note that for $J_2 - J_1 > 0$, negative entropy production βD (the entropy reduction) is associated with the positive information production I , which should be now referred to as the information creation rather than loss.

We have studied fluctuations of the flux difference $J_2 - J_1$, which is the time derivative of the variable $X_2 - X_1$. This variable characterizes not energy but the degree of organization of the system. In the case of the macroscopic mechanical machines, it could be, for example, the possibly slipping angle of a component wheel to axle. In the case of a macroscopic battery (the electrochemical machine), it is the difference between the available electric charge and the unused amount of reductor, both quantities being determined in molecular units. Organization $X_2 - X_1$ is controlled by force A_2 . The main conclusion of our study is that the free energy processing has to be distinguished from the organization processing, what is schematically illustrated in fig. 12. Note that both free energy and organization are functions of the state of the system. As in the case of energy processing coupled to an information transfer considered in ref. [13], the reservoirs in fig. 12 include both environment and all the system's degrees of freedom besides these that determine its thermodynamic state.

For the systems operating under stationary isothermal conditions, the first and second laws of thermodynamics:

$$W_1 + W_2 = D \geq 0, \quad W_0 = D_0 \geq 0, \quad (17)$$

are fulfilled for the perfect free energy processing and loss, respectively. All the components of work W_1 , W_2 , and W_0 and dissipation D , and D_0 are functions of the process. In the perfect machine, the output flux is tightly coupled to the input flux, $J_2 = nJ_1$, and the output work is maximum. Dissipation D tends to zero when the perfect stationary machine works infinitely slow, $J_1 \rightarrow 0$, but then its input and output powers also drop to zero. Loss in the free energy processing means that no work on environment is performed despite the forced energy dissipation. Eq. (7) indicates that it occurs simultaneously with the information loss.

For the organization processing, the generalized first and second law can be written as

$$\beta D + I = C \geq 0. \quad (18)$$

Here, both the entropy production βD , the information production I , as well as C , the quantity which balances two former quantities and which could be referred to as the entire cost of the process, are also functions of the process.

For the macroscopic machines, there are no correlations between the fluxes, so that only the first component in (15) contributes to the information production I . In fact, it represents indirectly the entropy production in the hidden variable X_1 . For the macroscopic machines as well as the mesoscopic enzymatic machines with the single output gate, the information I and the direct entropy production βD must always be positive, of the same sign. Accordingly, I is to be interpreted as the information loss.

However, for the enzymatic machines with multiple output gates, we showed here (fig. 11) that the second component in (15) prevails over the first and I is of the opposite sign to βD . Only the free energy transducer, for which the works W_1 and W_2 are of the opposite sign, can be referred to as the machine. Similarly, only the organization transducer, for which the information production I and the entropy production βD are of the opposite sign, can be referred to as the organizer. For I being positive (the information creation), βD must be negative (the entropy reduction instead of production). The biological molecular machines, for which this is the case, may be said to act as Maxwell's demons, although they do not utilize the information creation for the performance of work.

Note that we do not distinguish the operating system and the memory as the previous investigators [7,8,9,10,11,12] did after the Szilard understanding of Maxwell's demon [2]. Rather, as in ref. [13], we treat the memory, contained in the internal dynamics of the machine, on an equal footing with the constraints and the heat bath, see fig. 12b.

When considering the coupling of the free energy donating process with the free energy accepting one, the case of the tight coupling, $J_2 - J_1 = 0$ with the reduction ratio $n = 1$, is exceptional. Our simulation clearly points out that such a case occurs for the total compensation of entropy production βD by information creation I , albeit, on the average, both tend then to zero (compare fig. 11). This case is the optimum in the sense that the organization cost C of the total process is then zero.

7 Possible biological implications

Two powerful tools of theoretical physics created at the turn of the century, the fluctuation theorem [30,31] and the dynamics of self-organized criticality [52,53], force a significant change of our views on the nature of the biological molecular machines action. Progress in the theory coincides with the intensive experimental and numerical studies of intrinsically disordered proteins [44,45,46,54].

A possible proposal, not to be underestimated, is that the structural memory, traditionally associated with DNA and RNA, can be complemented by a dynamical memory stored in the fluctuating transient states of the protein machines surrounded by its substrates. The transient stages of dynamics between the successive transitions through the input gate can last quite long [54,57,58], especially when more shortcuts and external transitions are taken into account [59]. Projection of the trajectory on the variable $X_2 - X_1$ has a form of time series representing continuous time random walk [54,57,58]. It is very likely, that the natively disordered transcription factors, in their one-dimensional search for the target intermittent by three-dimensional flights [60,61], perform not the passive diffusion but the active continuous time random walk.

As mentioned earlier [29], our approach is able to explain the observation, that the single myosin II head can take several steps along the actin filament per ATP molecule hydrolysed [37,38]. It is likely, that the mechanism of the action of the small G-proteins, which have a common ancestor with the myosin [62] and an alike partly disordered structure after binding the nucleoside triphosphate [63,64] is, after a malignant transformation, similar.

There are some arguments, for instance, for the kinesin motor [65,66,67,68], the cytoplasmic dynein motor [69,70], and the quinol:cytochrome c oxidoreductase [71,72], that a feedback control with the tight coupling is achieved in dimeric protein complexes, which are composed of two identical monomers. We have already ascertained, that this case is the optimum in the sense that the organization cost C of the total process is then zero. One can imagine such a process for a binary system, whose components a and b create and collect information alternately in such a way that the resultant information and entropy productions are zero (fig. 13). The cyclic, alternate behaviour is important for the corresponding cost could not to be assigned to individual components. In this respect, the model from fig. 13 differs essentially from the bipartite systems, intensively studied recently [11,12,42].

Similar considerations explain the tight coupling which takes place in a wide range of conditions for the trimeric F_1 ATPase rotary molecular motor [73]. To summarize, research of this kind could help to answer the certainly interesting question: why most protein machines operate as dimers or higher organized structures?

8 Conclusions and open problems

The main conclusion of the paper is that the free energy processing has to be distinguished from the organization

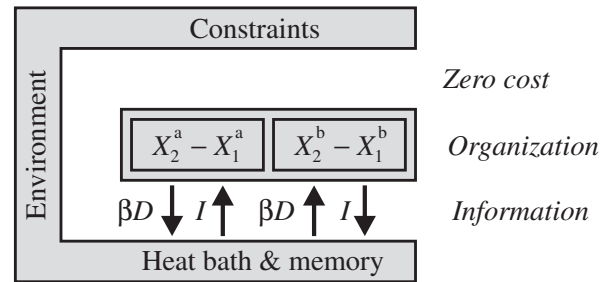


Fig. 13. Binary system whose components a and b create and collect information alternately in such a way that the resultant information and entropy productions are zero. Because the role of the components is indistinguishable, the cost of the process is zero.

processing. From the former point of view, Maxwell's demon utilizes entropy reduction ultimately for the performance of work, whereas from the latter, only for the creation of information. Our answer to the question posed in the title is that the biological molecular machines can, under certain conditions, act as Maxwell's demons, but only creating information, and not performing work.

We know, that work and heat are the changes of energy. We know also, that the internal entropy production is irreversibly transferred between the free and bound energy. But there is still controversy [74], the change of which physical quantity is information? Here, we suggest the answer, that information is the change of organization, a quantity being the difference of two physical quantities taking part in the free energy-transduction process. In such approach, the dual nature of entropy becomes clear as the physical quantity that connects the processes of free energy and organization transduction.

The first and second laws of thermodynamics (17) are valid in any conditions, whereas the first and second laws of organization transduction (18) were justified only for the stationary isothermal processes. The open problem remains generality of these laws. One thing is certain: the necessary conditions for the information and entropy productions to be of the opposite signs, is the presence of fluctuations and the possibility of a choice. Besides the mesoscopic machines, we know two macroscopic systems sharing such properties and intriguing long: detectors coupled to the critical fluctuations [75,76] or entangled with the quantum fluctuations [77,78,79].

Acknowledgements

We thank one of the anonymous referees of the previous version of the paper for valuable remarks. MK is also indebted to Yaşar Demirel and Hervé Cailleau for discussing the problem in the early stages of the investigation.

References

1. J. C. Maxwell, *Theory of Heat* (Logmans, London, 1871).

2. L. Z. Szilard, *Z. Phys.* **53**, 840 (1929).
3. R. Landauer, *IBM J. Res. Dev.* **5**, 183 (1961).
4. H. S. Leef, A. F. Rex, eds., *Maxwell's Demon 2: Entropy, Classical and Quantum Information, Computing* (Institute of Physics Publishing, Philadelphia, 2003).
5. K. Maruyama, F. Nori, V. Vedral, *Revs. Mod. Phys.* **81**, 1 (2009).
6. T. Sagawa, *Thermodynamics of Information Processing in Small Systems* (Springer, Berlin, 2013).
7. T. Sagawa, M. Ueda, *Phys. Rev. Lett.* **104**, 090602 (2010).
8. M. Pomurugan, *Phys. Rev. E* **82**, 031129 (2010).
9. T. Sagawa, M. Ueda, *Phys. Rev. Lett.* **109**, 180602 (2012).
10. D. Mandal, C. Jarzynski, *Proc. Natl. Acad. Sci. USA* **109**, 11641 (2012).
11. D. Hartich, A. C. Barato, U. Seifert, *J. Stat. Mech.* **14**, P02016 (2014).
12. J. M. Horowitz, M. Esposito, *Phys. Rev. X* **4**, 031015 (2014).
13. S. Deffner, C. Jarzynski, *Phys. Rev. X* **3**, 041003 (2013).
14. M. Smoluchowski, *Phys. Z.* **13**, 1069 (1912).
15. R. P. Feynman, R. B. Leighton, M. Sands, *The Feynman Lectures on Physics*, vol. 1 (Addison-Wesley, Reading, 1963), chap. 46.
16. C. Jarzynski, O. Mazonka, *Phys. Rev. E* **59**, 6448 (1999).
17. A. F. Huxley, *Prog. Biophys. Biophys. Chem.* **7**, 255 (1957).
18. J. Howard, in *Biological Physics – Poincaré Seminar 2009*, B. Duplainer, V. Rivasseau, eds. (Springer, Basel, 2010), pp 47-61.
19. J. M. Horowitz, T. Sagawa, J. M. R. Parrondo, *Phys. Rev. Lett.* **111**, 010602 (2013).
20. M. Kurzynski, *Prog. Biophys. Molec. Biol.* **69**, 23 (1998).
21. M. A. Fisher, A. B. Kolomeisky, *Proc. Natl. Acad. Sci. USA* **96**, 6597 (1999).
22. A. B. Kolomeisky, M. E. Fisher, *Annu. Rev. Phys. Chem.* **58**, 675 (2007).
23. D. Tsygankov, M. E. Fisher, *J. Chem. Phys.* **128**, 015102 (2008).
24. R. D. Astumian, I. A. Derenyi, *Biophys. J.* **77**, 993 (1999).
25. B. Bustamante, D. Keller, G. Oster, *Acc. Chem. Res.* **34**, 412 (2001).
26. R. Lipowsky, *Phys. Rev. Lett.* **85**, 4401 (2000).
27. R. Lipowsky, S. Liepelt, A. Valleriani, *J. Stat. Phys.* **135**, 951 (2009).
28. M. Kurzynski, P. Chelminiak, *J. Stat. Phys.* **110**, 137 (2003).
29. M. Kurzynski, M. Torchala, P. Chelminiak, *Phys. Rev. E* **89**, 012722 (2014).
30. C. Jarzynski, *Eur. Phys. J. B* **64**, 331 (2008).
31. U. Seifert, *Rep. Prog. Phys.* **75**, 126001 (2012).
32. J. M. R. Parrondo, J. M. Horowitz, T. Sagawa, *Nature Phys.* **11**, 131 (2015).
33. H. D. Rozenfeld, C. Song, H. A. Makse, *Phys. Rev. Lett.* **104**, 025701 (2010).
34. F. Escolano, E. R. Handcock, M. A. Lozano, *Phys. Rev. E* **85**, 021104 (2012).
35. T. L. Hill, *Free Energy Transduction and Biochemical Cycle Kinetics* (Springer, New York, 1989).
36. M. Kurzynski, *The Thermodynamic Machinery of Life* (Springer, Berlin, 2006).
37. K. Kitamura, M. Tokunaga, A. H. Iwane, T. Yanagida, *Nature* **397**, 129 (1997).
38. K. Kitamura, M. Tokunaga, S. Esaki, A.-H. Iwane, T. Yanagida, *Biophysics* **1**, 1 (2005).
39. D. Andrieux, P. Gaspard, *J. Stat. Phys.* **127**, 107 (2007).
40. C. Jarzynski, *Phys. Rev. Lett.* **78**, 2690 (1997).
41. J. Mehl, B. Lander, C. Bechinger, V. Blickle, U. Seifert, *Phys. Rev. Lett.* **108**, 220601 (2012).
42. N. Shiraishi, T. Sagawa, *Phys. Rev. E* **91**, 012130 (2015).
43. M. Borrelli, J. V. Koski, S. Maniscalco, J. P. Pekola, *Phys. Rev. E* **91**, 012145 (2015).
44. K. Henzler-Wildman, D. Kern, *Nature* **450**, 964 (2007).
45. J. D. Chodera, F. Noe, *Curr. Opin. Struct. Biol.* **25**, 135 (2014).
46. D. Shukla, C. X. Hernandez, J. K. Weber, V. S. Pande, *Acc. Chem. Res.* **48**, 414 (2015).
47. R. Zwanzig, *Acc. Chem. Res.* **23**, 148 (1990).
48. H. P. Lu, L. Xun, S. Xie, *Science* **282**, 1877 (1998).
49. A. M. van Oijen, P. C. Blainey, D. J. Crampton, C. C. Richardson, T. Ellenberger, X. S. Xie, *Science* **301**, 1235 (2003).
50. M. Kurzynski, *Cell. Molec. Biol. Lett.* **13**, 502 (2008).
51. X. S. Xie, *Science* **342**, 1457 (2013).
52. P. Bak, *How Nature Works* (Springer, New York, 1996).
53. K. Sneppen, G. Zocchi, *Physics in Molecular Biology* (Cambridge University Press, New York, 2005).
54. X. Hu, L. Hong, M. D. Smith, T. Neusius, X. Cheng, J. C. Smith, *Nature Phys.* **12**, 171 (2016).
55. K.-I. Goh, G. Salvi, B. Kahng, D. Kim, *Phys. Rev. Lett.* **96**, 018701 (2006).
56. P. Chelminiak, M. Kurzynski, preprint, arXiv:1512.04311 v1 (2015).
57. R. Metzler, *Nature Phys.* **12**, 113 (2016).
58. R. Metzler, J.-H. Jeon, A. G. Cherstvy, E. Barkai, *Phys. Chem. Chem. Phys.* **16**, 24128 (2014).
59. M. Kurzynski, P. Chelminiak, *Entropy* **16**, 1962 (2014).
60. A. Tafvizi, F. Huang, A. R. Ferhst, L. A. Mirny, A. M. A. van Oijen, *Proc. Natl. Acad. Sci. USA* **108**, 263 (2011).
61. G.-W. Li, X. S. Xie, *Nature* **475**, 308 (2011).
62. F. J. Kull, R. D. Vale, R. J. Fletcher, *J. Muscle Res. Cell Motil.* **19**, 877 (1998).
63. H. Houdusse, H. L. Szent-Györgi, C. Cohen, *Proc. Natl. Acad. Sci. USA* **97**, 11238 (2000).
64. I. Kosztin, R. Bruinsma, P. O'Lague, K. Schulten, *Proc. Natl. Acad. Sci. USA* **99**, 3575 (2002).
65. M. Bier, *Biosystems* **88**, 301 (2007).
66. R. D. Astumian, *Biosystems* **93**, 8 (2008).
67. S. Liepelt, R. Lipowski, *Phys. Rev. E* **79**, 011917 (2009).
68. R. D. Astumian, *Biophys. J.* **98**, 2401 (2010).
69. D. Tsygankov, A. W. R. Serohijos, N. V. Dokholyan, T. C. Elston, *J. Chem. Phys.* **130**, 025101 (2009).
70. D. Tsygankov, A. W. R. Serohijos, N. V. Dokholyan, T. C. Elston, *Biophys. J.* **101**, 144 (2011).
71. M. Świerczek, E. Cieluch, M. Sarewicz, A. Borek, C. Moser, P. L. Dutton, A. Osyczka, *Science* **329**, 451 (2010).
72. M. Sarewicz, A. Osyczka, *Physiol. Rev.* **95**, 219 (2015).
73. E. Gerritsma, P. Gaspard, *Biophys. Revs. Lett.* **5**, 163 (2010).
74. J. P. Crutchfield, *Nat. Phys.* **8**, 17 (2012).
75. P. W. Anderson, *Science* **177**, 393 (1972).
76. R. G. Palmer, *Adv. Phys.* **31**, 669 (1982).
77. W. H. Zurek, *Revs Mod. Phys.* **75**, 715 (2003).
78. W. H. Zurek, *Nature Phys.* **5**, 181 (2009).
79. P. Gaspard, *Phys. Lett. A* **377**, 181 (2013).